Centrifuge Modelling of Tunneling-Induced Settlement Damage to 3D-Printed Surface Structures

S. Ritter[1]; G. Giardina[2]; M.J. DeJong[3]; R.J. Mair[4]

[1] PhD Researcher, University of Cambridge, Department of Engineering, CB2 1PZ Cambridge, United Kingdom, sr671@cam.ac.uk

[2] Research Associate, University of Cambridge, Department of Engineering, CB2 1PZ Cambridge, United Kingdom, gg376@cam.ac.uk

[3] Senior Lecturer, University of Cambridge, Department of Engineering, CB2 1PZ Cambridge, United Kingdom, mjd97@cam.ac.uk

[4] Professor, University of Cambridge, Department of Engineering, CB2 1PZ Cambridge, United Kingdom, rjm50@cam.ac.uk

ABSTRACT

For urban tunneling projects it is essential to predict and prevent building damage. Although various case studies and experiments have shown that buildings considerably modify greenfield soil movements, widely accepted damage assessment methods neglect this soil-structure interaction and simplify structures as linear elastic beams. This paper summarizes an experimental investigation of the response of more realistic structures to tunneling-induced deformations. Small scale structural models with façade openings and brittle material properties were 3D printed and tested in a geotechnical centrifuge. Soil and structure displacement data were obtained by image-based measurement. Results demonstrate that structures notably mitigate differential greenfield ground displacements. It is also shown that maximum soil settlements, horizontal soil displacements beneath the structure and structural damage in the form of cracking significantly depend on the position of the structure in the settlement profile. The results provide a basis from which to predict building settlement response with greater certainty.

INTRODUCTION

With continuing population growth and increasing urbanization expected in the next decades, there is an urgent need for a next generation of infrastructure. It is likely that a large part of this infrastructure will be underground. Such creation of urban underground space frequently involves the excavation of shallow tunnels in close proximity to existing structures and utilities. For example, along the Crossrail project in London more than 1,200 structures are located within a possible influence area of the tunnel construction (Torp-Petersen and Black 2001). The assessment of building damage plays a vital role throughout the planning, design and construction stage of urban tunneling projects. However, while predictions of tunneling-induced deformations in the greenfield can generally be made with some confidence, much uncertainty exists about how structures interact with ground movements arising from tunnel construction.

The damage assessment procedures widely applied in practice commonly neglect any interaction between the soil and the structure, and thus it is assumed that the surface structures follow the greenfield displacements. Another simplification is that buildings are modelled as elastic beams (Burland and Wroth 1974). As a consequence, these methods generally tend to over predict potential building damage which can increase tunnel project costs.

Within the last two decades, a considerable amount of research has been carried out on the influence of the building stiffness on this tunnel-soil-structure interaction problem. Notable studies include Potts and Addenbrooke (1997), Son and Coording (2005), Franzius et al. (2006), Farrell (2010) and Goh and Mair (2012). Based on this research, alternative building damage assessment methods have been developed, which relate the stiffness of the structure to the soil stiffness. While the effect of the building stiffness on tunneling-induced ground movements has received considerable attention, much less is known about other factors influencing this soil-structure interaction problem. As an example, numerical simulations (Liu et al. 2000) , experimental tests (Al Heib et al. 2013 and Nghiem et al. 2014), and field data (Dimmock and Mair 2008) have shown that the transfer of ground displacements to masonry facades depends on the position of the structure relative to the tunnel. However, there is little agreement on how to incorporate the building dimensions or location of the building relative to the tunnel in these relative stiffness approaches. Dimmock and Mair (2008) proposed to account for the building location through considering only the building foundation when calculating the relative stiffness of masonry structures in hogging, but there is a general lack of data to refine the procedures to incorporate the building location when predicting damage. In addition, previous experimental studies paid little attention to replicating full-scale soil behavior or used very simple building models. The purpose of this work is to provide experimental data regarding the effect of the position of the structure within the tunneling-induced settlement trough that will enable improved relative stiffness damage predictions. In the process, the ground response beneath the structure and building cracking damage were also investigated. A series of centrifuge tests are presented which model a complex plaster-based 3D printed surface structure subjected to the influence of tunneling in sand.

EXPERIMENTAL METHOD

While field data from real tunnel projects provide important insights into the soil-structure interaction problem, experimental testing allows one to study the variation of key parameters in a controlled laboratory environment. However, the soil behavior is highly non-linear and depends on the confining stress. Centrifuge modelling enables the simulation of full-scale ground stresses, and thus more realistic soil behavior, when testing small scale models. This is achieved through increasing the gravity acting on the small-scale model within a centrifuge by a factor N, while the model is geometrically scaled down by the same factor.

Centrifuge Model

For this research, three tests were conducted in the 10 m diameter beam centrifuge at the University of Cambridge. Additionally, greenfield data from a centrifuge test performed by Farrell (2010), who used an equivalent experimental setup, is used for comparison. The tests were performed at 75 times the earth gravity field (75g). Figure 1 illustrates the centrifuge model and its main dimensions. The paragraphs below describe the main components and techniques used.

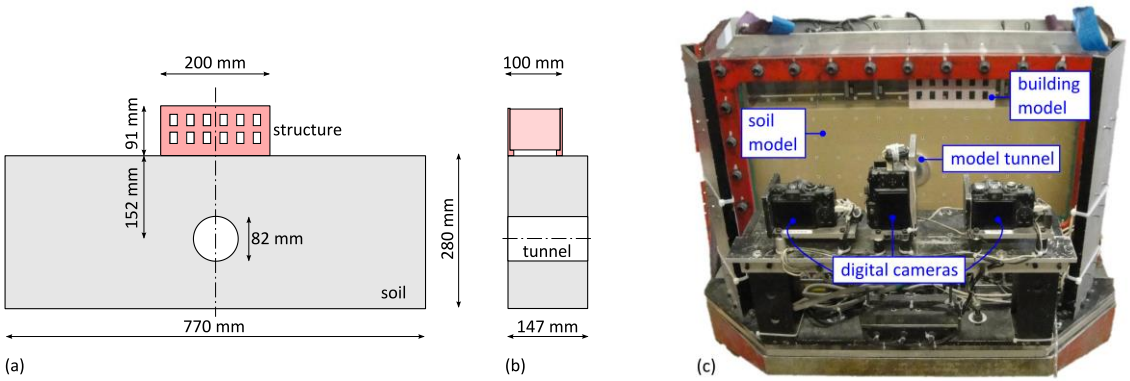

Figure 1: Centrifuge model configuration: (a) schematic front view, (b) cross-section through tunnel centerline, and (c) front view of centrifuge model configuration

Soil Model. For the entire centrifuge test series, Leighton Buzzard Fraction E sand was poured to achieve a uniform soil model with a relative density of about 90%. Typical properties of this dry silica sand are a D_{50} grain size of 0.14 mm, a specific gravity of 2.65, minimum and maximum void ratios of 0.613 and 1.014, and a critical state friction angle of 32° (Haigh and Madabhushi 2002).

Model tunnel. The model tunnel consists of a brass cylinder which is sealed with a flexible latex lining. The annulus between the brass cylinder and the latex membrane is filled with water. Schematic tunnel excavation in terms of tunnel volume loss is simulated through withdrawing a controlled amount of water from the tunnel. For more details on the design of the model tunnel see Marshall et al. (2012).

Surface Structures. In order to study the response of masonry surface structures, building models were 3D printed (Figure 2). A *Zprinter350* 3D printer with *Visijet PXLCore* powder and *Visijet PXLClear* binder was used. There are two benefits of this plaster-based 3D printing technique: (a) to create small-scale building models which are capable of cracking, and that (b) have realistic building characteristics such as foundations, façade openings, and intermediate walls. The building models are characterized by 20% of window openings, a rough soil-structure interface due to an unevenly printed foundation base, two intermediate walls and additional dead load resulting in a base interface stress of 100 kPa. A red texture was applied to the front façade of the building model to obtain image based deformation measurement. Chan (2012) reported that the building models had to be positioned close to the center of the print bed and the direction of flexural stress had to be aligned with the horizontal axis of the print bed to ensure repeatable 3D printer output. Considering these findings, the print space was significantly limited and two separate print jobs were necessary to print one building model as illustrated in Figure 2. The two 3D printed objects were subsequently glued together using common epoxy adhesive.

The main drawback of the used 3D printer is that the material properties of the 3D printed material cannot be modified by the user. To obtain the material properties of the 3D printed material, specimen with dimensions of 125 mm by 20 mm by 4 mm were 3D printed and tested in four-point bending. Table 1

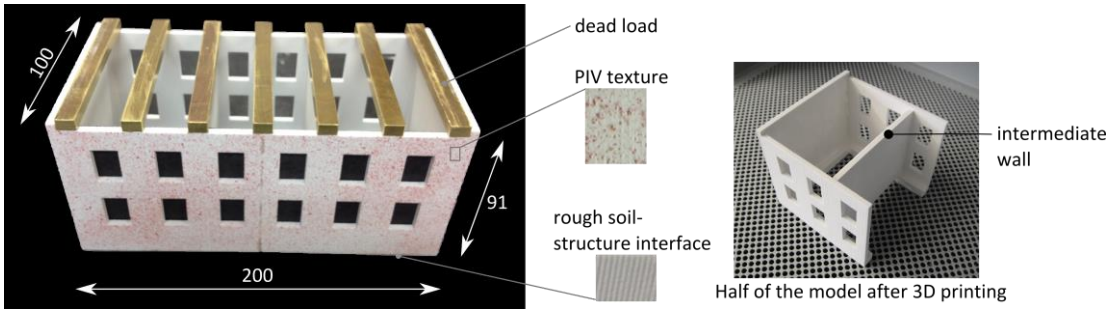

Figure 2: 3D printed building model. All dimensions in mm

gives an overview of the obtained material properties alongside of typical properties of masonry. Table 1 shows that while the 3D printed material is relatively brittle as desired, it is less stiff, stronger, and more ductile than typical masonry. As a result, cracking damage during the centrifuge experiments is expected at higher deformations than in prototype masonry structures. However, the building layout and the window opening percentage could be adjusted to create building models with bending ($1.3 \cdot 10^6$ kNm²/m) and axial stiffness ($5.0 \cdot 10^5$ kN/m) values comparable to a range of field cases (Dimmock and Mair).

Table 1: Material properties of 3D printed material compared to masonry properties from Giardina et al. (2015)

	Density ρ (g/cm³)	Young's modulus E (MPa)	Flexural strength f_t (MPa)	Strain to failure ε_f (%)
3D printed material	1.28	807.0	1.27	0.31
Masonry	1.9	1000 - 9000	0.1 – 0.9	0.05[ɨ]

[ɨ] Strain at onset of cracking for brick walls (Burland and Wroth 1974).

Image Based Deformation Measurement. The experimental results discussed in the subsequent sections were obtained through Particle Image Velocimetry (PIV), an image based deformation measurement technique (White et al. 2003). Three digital cameras were mounted in front of the Perspex window to capture images of the soil and the structure as shown in Figure 1c. The images were acquired at defined increments of the tunnel excavation simulation. As a result, measured soil and structure displacements within the Perspex plane can be related to a specific tunnel volume loss.

Urban Tunneling Scenarios. Figure 3 shows the urban tunneling scenarios modelled, which replicate a prototype tunnel project with a tunnel diameter of 6.2 m, a cover of about 8.3 m, and a 2-storey surface structure. While keeping the building and soil characteristics constant, the building location relative to the tunnel varied for every test. The three locations are denoted C1, C2 and C3. The location of the structure in the settlement profile can be defined by its eccentricity (e), which is defined as the distance between the mid-point of the structure and the tunnel centerline. The structure in C1 (Figure 3a) is mainly located within the sagging region of the greenfield settlement trough where compression strains are predominant. In contrast, the structure in C2 (Figure 3b) is placed within the tension or hogging zone of the greenfield settlement profile. Figure 3c illustrates the final tunneling scenario modelled with a structure placed in the transition zone between hogging and sagging (C3). The transition between hogging and sagging is defined by the inflection point, which is the location of the maximum slope of the settlement trough.

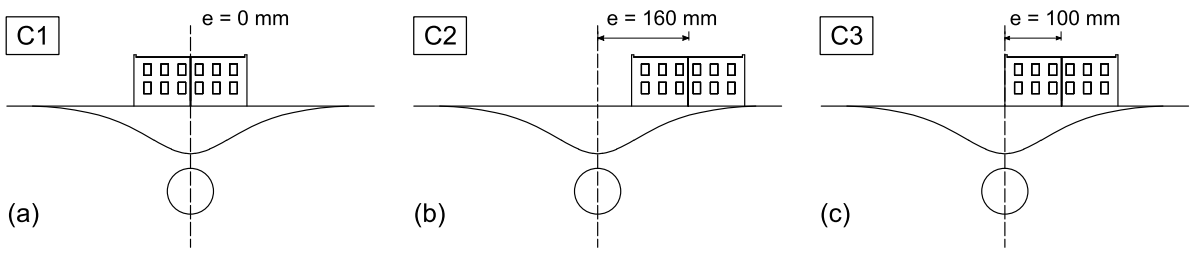

Figure 3: Centrifuge modelling test series: (a) case C1 with a structure in sagging, (b) case C2 with a structure in hogging, and (c) case C3 with a structure in the transition zone

GROUND RESPONSE

This section describes and discusses the response of the soil beneath the building models.

Volume Loss

While ground movements of tunnels in undrained clay show constant volume conditions, tunnels in drained soils (i.e. sand and gravels) show different volumetric behavior (Marshall et al. 2012). Figure 4 compares the soil volume loss measured near the soil surface with the tunnel volume loss for the performed centrifuge tests. This figure shows that the surface soil volume loss significantly differs from the simulated tunnel volume loss. These results are in line with previous research by Marshall et al. (2012), who proposed the relationship between surface and tunnel volume loss that is included in Figure 4. The decrease of volume loss closer to the soil surface can be attributed to the volumetric behavior of dense sand during shear deformation. In particular, for the discussed tunneling scenario with a very low overburden, high shear strains cause dilation in the soil above the tunnel, and thus volume loss decreases closer to the soil surface. An implication of this finding is that the surface soil volume loss measured at the surface can differ considerably to the volume loss the tunnel is experiencing. This result is in particular true for relatively high tunnel volume losses. For example, for the tunneling scenario modelled, a tunnel volume loss of 2.0% is equivalent to a measured surface soil volume loss of about 1.6%, as indicated in Figure 4. At surface soil volume losses below 1.0%, which are frequently reported in tunneling practice, the difference becomes less striking.

What is interesting in the data of Figure 4 is that after a tunnel volume loss of about 1.5% is reached, the surface soil volume loss of the sagging scenario (C1) becomes considerably lower than the greenfield prediction. A possible explanation for this might be the formation of a gap beneath the center of the building and the soil, which reduces the mean soil stress and hence increases the rate of dilation. By contrast, there is a good agreement between the surface soil volume loss of the tests C2 and C3 and the greenfield prediction. These results are in line with the findings of Potts and Addenbrooke (1997), who reported that structures have a minor impact on the surface soil volume loss.

As Marshall et al. (2012) pointed out, tunnel volume loss cannot be directly measured in practice. However, the tunnel volume loss can be well controlled during centrifuge experiments and thus is a convenient parameter for centrifuge modelers. Therefore, the data presented below is related to the tunnel volume loss. Although tunnel volume losses of 2.0% or 4.0% seem to be unrealistic, the reader should bear in mind that the engineering volume loss measured at soil surface is notably smaller.

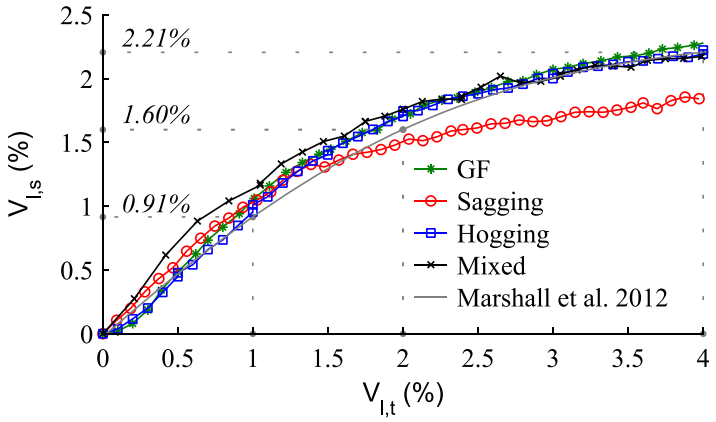

Figure 4: Variation of surface soil volume loss ($V_{l,s}$) with tunnel volume loss ($V_{l,t}$)

Vertical Soil Displacements

The displacement data below is given in model scale to account for the experimental nature of this research. A scale factor of 75 should be applied to translate the data into prototype scale. Figure 5 provides vertical surface soil displacement profiles at tunnel volume losses of 0.5%, 1.0%, 2.0% and 4.0%. Greenfield settlement profiles (Farrell 2010) at equivalent tunnel volume losses are included for comparison. It is evident from Figure 5 that the presence of the buildings changes the shape of the settlement troughs.

Figure 6 shows more in detail the effect of the building position on the vertical ground response at a tunnel volume loss of 2.0%. Figure 6a shows a local increase of the greenfield settlements directly beneath the edges of the structure placed in the symmetric position (C1). In contrast, the buildings in the positions C2 and C3 increase the greenfield settlements beneath the entire extent of the building (Figure 6b and c). This difference can be explained by a gap formation between the soil and the center of the structure in the sagging position. As a consequence of this reduced building footprint, the building weight redistributes to the edges of the structure and causes the structure to embed (Farrell and Mair 2012). This embedment considerably modifies the greenfield settlement profile at the trough shoulders (Figure 6a). As a result of this gap formation and building weight redistribution, the surface soil settlements above the tunnel centerline are considerably reduced compared to the greenfield scenario. This might be explained due to a decrease of the mean stress beneath the center of the structure which increases the amount of dilation in the soil body directly above the tunnel. A slight reduction of the greenfield settlements above the tunnel was also found for the structure in the hogging zone (Figure 6b). By contrast, Figure 6c shows that the structure positioned in the transition region increased the greenfield settlements above the tunnel. This can be explained by the rigid response of the building, with considerable tilt resulting in maximum surface soil settlements at the corner of the structure directly above the tunnel centerline.

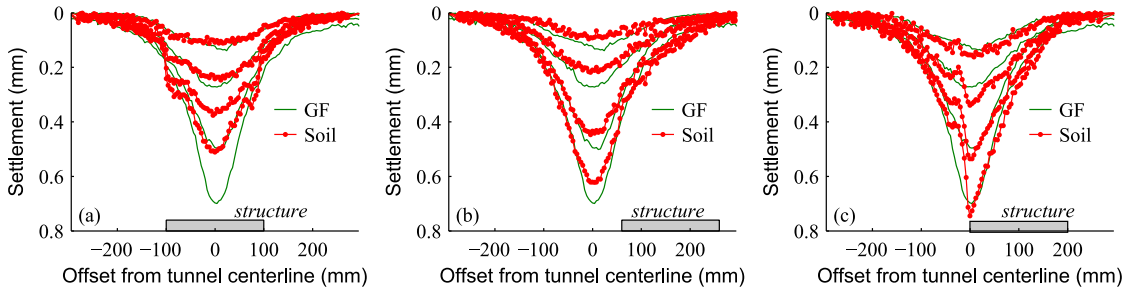

Figure 5: Surface settlement profiles for (a) structure in sagging, (b) structure in hogging, and (c) structure in the transition zone

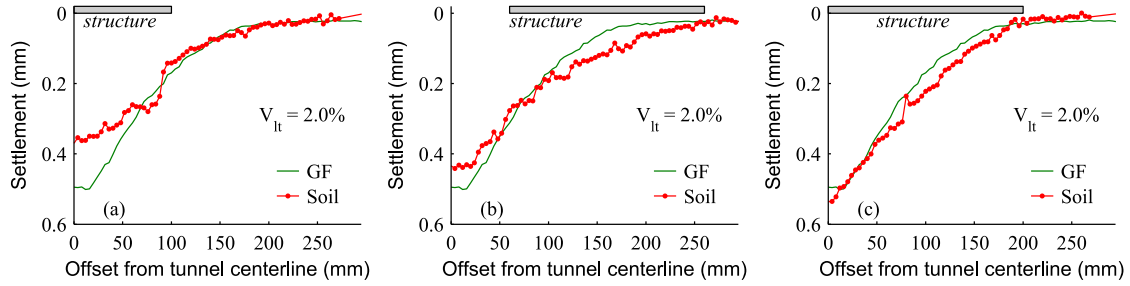

Figure 6: Vertical ground movements at a tunnel volume loss of 2.0% beneath (a) structure in sagging, (b) structure in hogging, and (c) structure in the transition region

The most striking result however is that the magnitude of differential soil settlements is considerably reduced beneath the structures compared to the greenfield case. This finding implies that neglecting soil-structure interaction might result in conservative assumptions when predicting settlement-induced building damage.

Horizontal Soil Displacements

Figure 7 shows the horizontal displacement of the soil surface measured directly beneath the structure for the three different building positions and tunnel volume losses of 0.5%, 1.0%, 2.0% and 4.0%. These displacement profiles are associated with the settlement profiles illustrated in Figure 5. For all building locations, the restraining influence of the structure on the horizontal surface displacements is clearly visible. This indicates that friction at the soil-structure interface reduces horizontal soil displacements.

However, varying eccentricity of the building results in different phenomena. Figure 7a and Figure 8a show that the horizontal surface soil displacements beneath the edge of the structure in sagging are significantly lower than the greenfield equivalents. By contrast, the horizontal displacements beneath the center area of the structure match the greenfield horizontal displacements. This can be explained by the gap formation (see above), which prevents the transfer of shear stresses between the soil and the structure. As a consequence, the soil moves freely beneath the center of the structure after the contact between the soil and the structure is lost. When the building is located non-symmetrically about the tunnel centerline, the horizontal soil displacements exhibit a nearly constant value beneath the entire structure (Figure 8b and c). For both building locations the measured horizontal soil displacements beneath the building exceed the greenfield equivalents towards the right hand side of the structure. This is due to the transfer of shear stresses from the building to the soil, which causes the soil beneath the structure to follow the horizontal displacement of the structure. For all sets of building locations, the greenfield horizontal displacements are recovered after about 25% of the length of the structure.

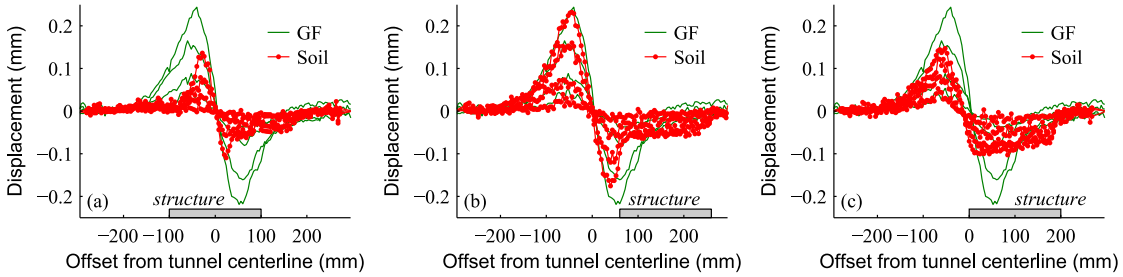

Figure 7: Horizontal soil surface displacements beneath (a) structure in sagging, (b) structure in hogging, and (c) structure in the transition region

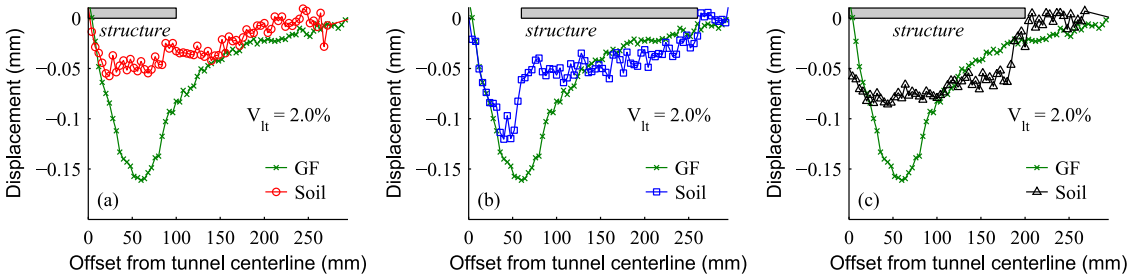

Figure 8: Horizontal surface ground response at a tunnel volume loss of 2.0% for (a) a structure in sagging, (b) a structure in hogging, and (c) a structure in the transition region

BUILDING DAMAGE

The final part of this paper discusses the transfer of the ground movements to the structure and associated building damage. Figure 9 compares the vertical displacements of the base of the structure to the greenfield settlement profiles (Farrell 2010) at a tunnel volume loss of 2.0%. Figure 9 shows that the stiffness of the structure prevented the greenfield ground displacements from being transferred to the structure. When the building was placed symmetrically to the tunnel (C1), the structure deformed purely in sagging (Figure 9a). Although great care was taken during model preparation, local differences in the soil model caused the building in C1 to tilt slightly. The structure in C2 deformed purely in hogging while the structure in C3 performed mainly in hogging with a minor sagging response close to the tunnel. As expected, the structure in the transition zone (C3) experienced the greatest tilt (Figure 9c).

Figure 10 presents the horizontal displacements at the base of the building models. Greenfield displacements (Farrell 2010) and soil response are illustrated for comparison. For all building locations, negligible horizontal displacements are transferred to the structure. Figure 10 highlights this observation by also presenting the associated very small horizontal building strains (at the base of the structure, averaged over the entire length). These were determined from the slope of a linear function fitted to the horizontal structure displacements. The results, however, show differences caused by the location of the building. In the hogging case (C2), the building is located in the area where the soil imposes tensile horizontal movements to the base of the building. Although the structure significantly reduces the greenfield horizontal soil displacements, very minor average horizontal tension strains are transferred to the base of the structure (Figure 10b). When the structure is placed in sagging (C1), the ground tends to impose average horizontal compression strains to the base of the building (Figure 10a). This demonstrates that the compressive horizontal ground movements dominate over any potential tensile

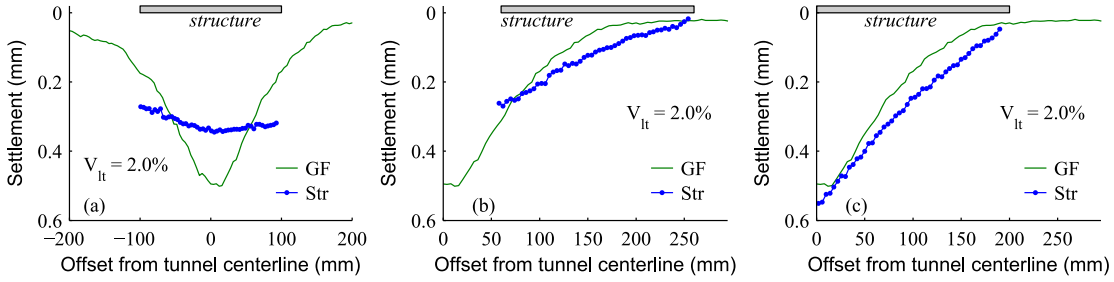

Figure 9: Vertical structure response for (a) structure in sagging, (b) structure in hogging, and (c) structure in the transition zone

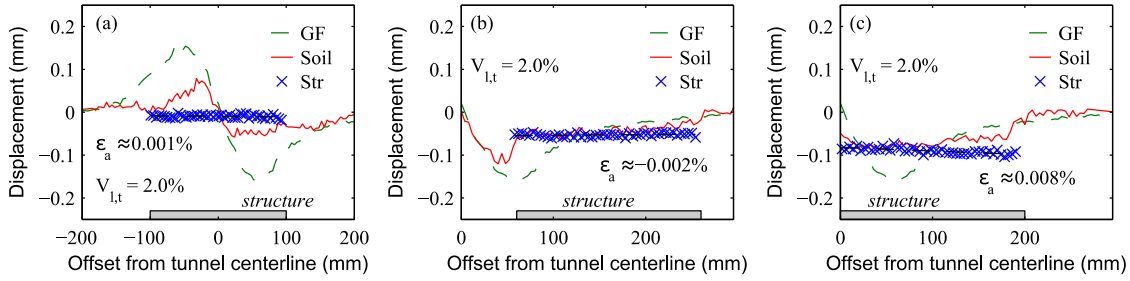

Figure 10: Horizontal movement at the base of the structure at a tunnel volume loss of 2.0% for (a) structure in sagging, (b) structure in hogging, and (c) structure in the transition region. Average horizontal strains over the length of the structure at its base are also shown inset (compressive strains are positive).

strains due to bending in the sagging region. Interestingly, the average horizontal base strain of the building in the transition region (C3) is also compressive (Figure 10c). While the left part of the base of the building is slightly restrained due to the reduction of horizontal ground movements above the tunnel, the right part of the base of the structure is horizontally pushed towards the center; thus, the measured average horizontal strain within the base of the building is compressive.

Visible cracking in the building models, measured through PIV, is illustrated in Figure 11. Whereas cracking was observed for the buildings in hogging (C2) and the transition region (C3), the structure in sagging stayed intact. As noted above, the 3D printed material is stronger and considerably less brittle than real masonry, and hence visible cracking occurred at unrealistically high tunnel volume losses. Micro-cracks might have developed at lower tunnel volume losses, which will be explored in future research. Figure 11 shows that for the structures in hogging (C2) and the transition region (C3) cracking developed at a tunnel volume loss of about 14.7% and 8.25%, respectively. Despite the unrealistically high volume losses, these results indicate that buildings in the transition zone are most vulnerable to building damage in terms of cracking, which is consistent with findings of Nghiem et al. (2014). For both building locations, the cracks developed from the top to the bottom of the structure and were located close to the window corners as shown in Figure 11.

CONCLUSIONS

Centrifuge modelling of 3D printed structures provided new insight into the response of surface buildings to tunneling in sand. Three different building locations relative to the tunnel were explored. The experiments confirmed that the presence of the structure significantly modifies the greenfield soil displacements. Results show that a structure located symmetrically to the tunnel notably reduces the soil vertical displacements while a structure placed partially above the tunnel increases the soil settlements above the tunnel. Differential horizontal soil displacements beneath the structure are significantly reduced for all sets of building eccentricity. However, structures in the hogging and transition region can increase the horizontal greenfield soil displacements towards the building corner farthest from the tunnel.

For all three building locations, the structure behaved relatively rigidly and very small horizontal strains were transferred to the buildings. The structure in the transition zone was most vulnerable to cracking. The structure in the hogging region also experienced damage due to cracking while the structure located symmetrically to the tunnel showed no visible damage. The findings of this study provide the framework to refine the procedures for predicting tunneling-induced settlement damage.

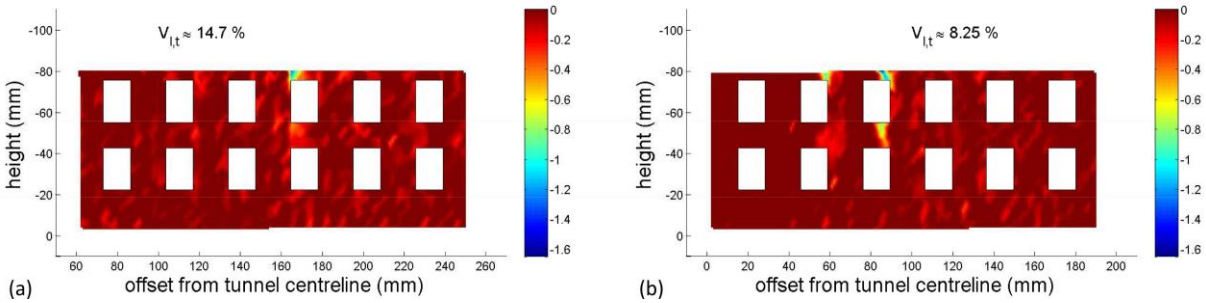

Figure 11: Horizontal building strains indicating building damage in terms of cracking for (a) a structure in hogging and (b) a structure in the mixed region. Tension strains are negative while compression is positive.

ACKNOWLEDGMENTS

The authors are grateful to Crossrail and EPSRC (EP/K018221/1) for funding this research, and to Dr Ruadhri P. Farrell for sharing experimental data. The associated research data can be accessed at https://www.repository.cam.ac.uk/handle/1810/253135.

REFERENCES

Al Heib, M., Emeriault, F., Caudron, M., Nghiem, L., and Hor, B. 2013. Large-scale soil–structure physical model (1g)–assessment of structure damages. In International Journal of Physical Modelling in Geotechnics, 13(4), 138-152.

Burland, J.B. and Wroth, C.B. 1974. Settlement of buildings and associated damage, Pentech Press, 611-54.

Chan, D.Y.K, 2012. 3D printing of structural scale models. Research report, Cambridge University.

Dimmock, P. S., and Mair, R. J. 2008. Effect of building stiffness on tunnelling-induced ground movement. Tunnelling and Underground Space Technology, 23(4), 438-450.

Farrell, R.P. 2010, Tunnelling in sands and the response of buildings. Diss. University of Cambridge.

Farrell, R.P., and Mair, R.J. 2012. Centrifuge modelling of the response of buildings to tunnelling. In Geotechnical Aspects of Underground Construction in Soft Ground-Proceedings of the 7th International Symposium, CRC Press, 343-351.

Franzius, J. N., Potts, D. M., and Burland, J. B. 2006. The response of surface structures to tunnel construction. In Proceedings of the ICE-Geotechnical Engineering, 159(1), 3-17.

Goh, K.H., and Mair, R.J. 2012. The response of buildings to movements induced by deep excavations. In Geotechnical Aspects of Underground Construction in Soft Ground-Proceedings of the 7th International Symposium, CRC Press, 903-910.

Giardina, G., Hendriks, M.A., and Rots, J.G. 2015. Sensitivity study on tunnelling induced damage to a masonry façade. Engineering Structures, 89, 111-129.

Haigh, S.K., and Madabhushi, S.G. 2002. Dynamic centrifuge modelling of the destruction of Sodom and Gomorrah. In International Conference on Physical Modelling in Geotechnics, AA Balkema, 507-512.

Liu, G., Houlsby, G.T., and Augarde, C.E. 2001. 2-dimensional analysis of settlement damage to masonry buildings caused by tunnelling. In Structural Engineer, 79(1), 19-25.

Marshall, A.M., Farrell, R.P., Klar, A., and Mair, R.J. 2012. Tunnels in sands: the effect of size, depth and volume loss on greenfield displacements. Géotechnique, 62(5), 385-399.

Nghiem, L., Al Heib, M., and Emeriault, F., 2014. Understanding subsidence consequences on masonry structures using large small-scale physical modeling. In 8. International Conference on Physical Modelling in Geotechnics (ICPMG 2014), CRC Press, 1195-1202.

Potts, D. M., and Addenbrooke, T. I. 1997. A structure's influence on tunneling-induced ground movements. Proceedings of the ICE - Geotechnical Engineering, 125(2), 109-125.

Son, M., and Cording, E. J. 2005. Estimation of building damage due to excavation-induced ground movements. Journal of Geotechnical and Geoenvironmental Engineering, 131(2), 162-177.

Torp-Petersen, G.E., and Black, M.G. 2001. Geotechnical investigation and assessment of potential building damage arising from ground movements: CrossRail. In Proceedings of the ICE-Transport. 147(2), 107-119.

White, D.J., Take, W.A., and Bolton, M.D. 2003. Soil deformation measurement using particle image velocimetry (PIV) and photogrammetry. Geotechnique, 53(7), 619-631.